Mr. D. Uday Bhaskar[1,*],
Mr. T. Papi Naidu[2]

Application of Super Conductor Magnetic Energy Storage System and FACTS Devices for a Two Area Load Frequency Control Containing Synchronous Generators and DFIG Wind Generator System

JES

Journal of Electrical Systems

The load change in a synchronous generator (SG) based power generation system is common which will mainly influence the change in voltage, power flows, frequency, load angle and burden o transmission lines and transformer due to change in current flow. The study which analyses the behavior of load change, compensating devices and its impact on change in frequency and real power flow is termed as load frequency control. The generators like Doubly Fed Induction Generator (DFIG), SG are supplying power in one area and total two areas are considered in this paper. The load change is done in area-1 only and change in frequency is observed in both areas. Three cases, one with thyristor controlled capacitor storage phase shifters (TCPS) and other with superconducting magnetic energy storage system (SMES) and a hybrid of these is done and in other case, FACTS devices like TCPS, SSSC, UPFC and IPFC are used. Using MATLAB software, the frequency change is observed in all the three cases, in the first case, TCPS is found better and in the second case, IPFC is found better in compensating the frequency change. In the third case, the frequency deviation is observed with coordinated devices SMES-SMES, SMES and TCPS and SMES and SSSC. It is found that SMES and SSSC coordinated device structure is best among all in terms of frequency deviation.

Keywords: load frequency control; DFIG; SMES; TCPS; SSSC; IPFC; UPFC; hybrid devices.

1. Introduction

The power system main components are generating stations, transmission lines, distribution lines, load centers and industrial and sub-station load management units. The generating stations play a key role in supplying load reliably and effectively to the load centers without voltage or frequency disturbance. The distribution and transmitting stations supply real power at desired voltage and frequency to industrial, commercial and domestic loads such that the deviation in voltage and frequency with respect to rated to be as lesser as possible. If there is a deviation in voltage or frequency due to load disturbances, the performance and the life of motors and lighting loads deteriorate. To overcome this, the distribution, transmission and generating stations control the frequency such that the deviation in frequency is as low as possible last few decades [1, 2].

The load frequency control is done on distribution generation model is done for low and medium power level applications where generator speed control and model based control techniques are widely used [3-6]. There are various advanced control schemes such as adaptive reference models, intelligent fuzzy, neural networks, and meta-heuristic techniques like GA, PSO etc., are used [7-10]. These advanced controllers are very quicker and can predict the load changes and can adapt to the system behavior as per the requirements. Other than controllers, compensating devices like energy storage and FACTS devices are crucial for system performance and stability improvement [11-18]. These devices will supply or absorb real or reactive power to the load system where installed to meet the change in the demand. Mostly, batteries, fuel-cell, capacitors are used to supply

---

* Corresponding author: Mr. D. Uday Bhaskar, Lendi Institute of Engineering & Technology, Jonnada, Vizianagaram, Andhrapradesh, India, E-mail: udaybhaskard222@gmail.com

[1] Lendi Institute of Engineering & Technology, Vizianagaram-535005

[2] Associate Professor, Department of EEE, Lendi Institute of Engineering & Technology, Vizianagaram-535005

real power when load increases and absorb when load decreases. The inverter which connects these dc supply energy sources to ac grid will control reactive power flow. The FACTS devices are controlled voltage and current control switches like IGBTs, SCRs. The FACTS devices include thyristor controlled capacitor storage phase shifters (TCPS), STATCOM, SSSC, IPFC, UPFC, and SVC are used for voltage, frequency, load angle and reactive power flow compensation.

There are three hierarchical frequency controls, namely, primary, secondary and tertiary controls [19-21]. The governor action for the generator-turbine that is responsible for fuel input and thereby frequency control is called primary frequency control. This will maintain the generator station side overall frequency stability, balancing power between generation and the load. The Automatic Generation Control (AGC) is the control level for two or more areas in a large power system, which is said to be secondary level of frequency control. The frequency level control between the main grid and the micro-grid is said to be tertiary control. The knowledge on all these levels of control helps in effective design control of LFC [16]. The natural frequency response in a power system refers to the combined effect on generator and AGC's [6].

In this paper, three cases are discussed with first case load change in area-1 only for frequency compensation, one with SMES, other with only TCPS and also a hybrid of these SMES and TCPS. In the other case, TCPS, SSSC, UPFC and IPFC devices are used and the frequency compensation is discussed. In the final case, coordinated FACTS and energy storage devices are placed in each area and the frequency deviation is examined. To find the better device among these in terms of frequency compensation, complexity of control and price are done. The second section discuses the area control error in a two area system mathematically, third section discuss the DFIG wind-turbine system performance based on load frequency concept. The fourth section discusses test bed under study and also the design of these energy and FACTS devices and later in fifth section observes the results and analyzes behavior during sudden load change. Finally, conclusions and major findings of the work are described.

2. Mathematical modeling of the two area system control error

The modification in the frequency because of load variation for a two area system is discussed in this section. The two areas are depicted with suffix A and B for easy understanding and the frequency control is as below. The composite frequency response (β_s) can be defined in terms of system governor droop function in (R_s) Hz per pu power and characteristic load damping (D_s) in pu power per Hz as [12]

$$\beta_s = \frac{1}{R_s} + D_s \tag{1}$$

The equation (1) helps to understand the frequency regulation in a multi-area power system. The natural response of the frequency restrains the variation in the frequency due to generation-load disparity, which requires an effective control. The steady-state frequency deviation in pu frequency (Δf) under active power imbalance (ΔP_L) in pu power is defined as

$$\Delta f = -\frac{\Delta P_L}{\beta_s} \tag{2}$$

The expression (2) refers to the primary level of frequency control. The Automatic Generation Control (AGC), based frequency level control is known as secondary or supplementary control that depends on two areas frequency control which restores tie-line system frequency to its supposed values. This control level plays a vital role controlling all the area's active power and frequency parameters and hence balances generation-load error

which is referred to as Area Control Error (*ACE*), in MW. The interconnected tie-line bias control (TBC) [7, 8] helps in regulating and balancing all the areas frequency independently. The *ACE* is computed in terms of actual (Ta) and scheduled (Ts) exchange power of the line and actual (f) and nominal (f0) system frequency based on balancing area frequency bias (B) according to:

$$ACE = (T_a - T_s) - 10B(f - f_0) \tag{3}$$

where *B* is a negative value in terms of MW/0.1Hz,. It is set to match the balancing area's frequency response coefficient, and must not be less than 1% of balancing area's estimated yearly peak demand per 0.1Hz change [9].

For two areas *A* and *B*, the *ACE* in each area is stated as:

$$ACE_A = (T_{Aa} - T_{As}) - 10B_A(f - f_0) \tag{4}$$

$$ACE_B = (T_{Ba} - T_{Bs}) - 10B_B(f - f_0) \tag{5}$$

Without loss of generality, under the assumption that all the line line power terms of the two areas are zero, given by $T_{Aa}\text{-}T_{As}=\text{-}(T_{Ba}\text{-}T_{Bs})$. This helps to find the frequency deviation using the equations (4) and (5), we have

$$f - f_0 = \frac{ACE_A + ACE_B}{-10(B_A + B_B)} \tag{6}$$

From the equation (6), we can conclude that, the change in the system frequency is directly proportional to vector sum of all the individual *ACE*s. Now the ACE is derived under TBC scheme in terms of power imbalance ΔP_L and individual areas composite frequency response is expressed as:

$$
\begin{aligned}
ACE_A &= (T_a - T_s) - 10B_A(f - f_0) \\
&= (-\Delta P_L + \Delta P_{GA} - \Delta P_{LA}) - 10B_A(f - f_0) \\
&= (-\Delta P_L - \beta_A \Delta f) - 10B_A \Delta f \\
&= -\Delta P_L - (\beta_A + 10B_A)\Delta f
\end{aligned}
\tag{7a}
$$

Further change in generation and load in area-A (ΔP_{GA}, ΔP_{LA}) as

$$\Delta P_{GA} = -\frac{1}{R_A}\Delta f, \ \Delta P_{LA} = D_A \Delta f \tag{7b}$$

The definition of steady-state frequency deviation $\Delta f = -\Delta P_L/\beta_S$ is used for ACE for both areas and solving for individual ACE using the above equations

$$ACE_A = \left(\frac{\beta_A + 10B_A}{\beta_s} - 1\right)\Delta P_L \tag{8a}$$

and,

$$ACE_B = \frac{\beta_B + 10B_B}{\beta_s}\Delta P_L \tag{8b}$$

where

$$B_A = \beta_A = \frac{1}{R_A} + D_A, \ B_B = \beta_B = \frac{1}{R_B} + D_B, \ \beta_s = \beta_A + \beta_B = \frac{1}{R_A} + \frac{1}{R_B} + D_A + D_B.$$

Based on the explanation given for equation (3) and (4) and reference number [9], $-10B_A = \beta_A$, $-10B_B = \beta_B$, we get $ACE_A = -\Delta P_L$ and $ACE_B = 0$

It means for the control of frequency in one area, i.e., AGC or ACE in area-A will react to its own power imbalance to meet the frequency response of the system, where ACE in area-B do not react, but will be a part in the governor and load frequency control response.

3. The DFIG wind turbine modeling based on load data

3.1 DFIG modeling based on load data

In this section, the deviation in the source to load real power change for the Doubly Fed Induction generation (DFIG) is discussed. The electromagnetic torque (EMT- T_e) developed by the DFIG in terms of moment of inertia is J, ω_r is rotor speed, B is friction coefficient, T_l is load torque [22]

$$T_e = J \frac{d\omega_r}{dt} + B\omega_r + T_l \tag{9a}$$

$$= (Js + B)\omega_r + T_l \tag{9b}$$

If multiplying with ω_{error} on both sides of equations to get the power parameters of DFIG can be expressed in terms of rotor angular speed (ω_r), speed error between reference to actual (ω_{error}) as

$$T_e\omega_{error} = (Js + B)\omega_r\omega_{error} + T_l\omega_{error} \tag{10}$$

We know that the product of speed and EMT is active power. Simplifying the equation (10) for reference stator power (P_s^*) in terms of the generator constants, we get the equation (11) as

$$P_s^* = (K_{in}s + K_{pn})\omega_{error} + P_l \tag{11a}$$

Now manipulating the power terms in equation (11) like stator output optimal reference power to load power (P_l) on to the left hand side and speed coefficient terms to the right hand side, we get equation (11b) as

$$P_s^* - P_l = (K_{in}s + K_{pn})\omega_{error} \tag{11b}$$

where, $K_{in} = J * \omega_r$ and $K_{pn} = B * \omega_r$

The equation (11b) describes the change in source power to load power and its effect on change in turbine rotor speed (ω_{error}).

3.2 The wind turbine modeling in a two area generation control

The electrical power output from the wind turbine-generator set is governed by the conversion of wind kinetic energy tnto mechanical energy by the turbine and further to the electrical energy by the generator. From the basic equations of wind energy conversion, mechanical output power (P_{mech}) from turbine is given by [12, 16 & 22]

$$P_{mech} = \frac{1}{2} C_p(\lambda, \beta)\rho A \upsilon_\omega^3 \tag{12}$$

Where wind power coefficient (C_p), ρ is specific density of air, R is radius of wind turbine blade, υ_ω is wind speed. The C_p is a function of pitch angle (β) and tip speed ratio (λ).

$$C_p(\lambda, \beta) = 0.645[0.00912\lambda + \left[\frac{116\lambda_t - 5 - 0.4(2.5 + \beta)}{e^{21\lambda_t}}\right] \tag{13}$$

$$\text{where,} \quad \lambda_t = \frac{1}{\lambda + 0.08(2.5 + \beta)} - \frac{0.035}{1 + (2.5 + \beta)^3} \quad \text{and} \quad \lambda = \frac{\omega_r R}{\upsilon_\omega} \tag{14}$$

The maximum mechanical power output from the wind turbine is defined as a function of mechanical power coefficient ($C_{p\ max}$), optimal wind or rotor speed (ω_{opt}) and turbine blade radius as

$$P_{\max} = \frac{1}{2\lambda_{opt}^3} \pi\rho C_{p\max} R^5 \omega_{opt}^3 \qquad (15)$$

Solving the equations from 12 to 14, Cp can be expressed as

$$C_p = \frac{1}{\dfrac{1}{\dfrac{R+\omega_r}{\upsilon_\omega}+0.08\beta} - \dfrac{0.035}{\beta^2+1}} \qquad (16)$$

Now the turbine and the generator modeling is expressed in terms of inertia constants to evaluate the effect the loading on the system [22]. The turbine, generator and system inertia constants (H_t, H_g and H_{sys}) as

$$2H_t \frac{d\omega_0}{dt} = T_m - K_{sh}\theta_s - D_{sh}(\omega_t - \omega_r) \qquad (17a)$$

$$2H_g \frac{d\omega_0}{dt} = -T_e + K_{sh}\theta_s + D_{sh}(\omega_t - \omega_r) \qquad (17b)$$

$$\frac{d\theta_s}{dt} = \omega_0(\omega_t - \omega_r) \qquad (17c)$$

$$2H_{sys} \frac{d\Delta f}{dt} + D\Delta f = P_g - P_\omega - P_L \qquad (17d)$$

$$\text{where } H_{sys} = \sum_{i=1}^n \frac{\dfrac{H_i\omega_{mi}^2}{2}}{S_{sys}} \qquad (17e)$$

ω_0, ω_r, ω_t, and ω_{mi} are the angular base speed, rotor speed, turbine speed before the gear box and rated mechanical rotor angular velocity of the ith generator. T_m and T_e are turbine and EMT of the DFIG. K_{sh}, D_{sh}, and θ_s are shaft stiffness, shaft damping constant and the torsion twist constants. N is number of the generators, Hi is the ith turbine-generator combined moment of inertia, S_{sys} is rated capacity of the entire power system network. From the equation (17e), we can conclude that as the penetration of wind resources (S_{sys}) increases, the inertia of the system (H_{sys}) decreases considerably. Now, the affect of percentage deloading (d%) on output generation of the DFIG (Pde) with respect to MPPT based real power generation of the DFIG is

$$P_{de} = (1 - d\%)P_{MPPT} \qquad (18)$$

The deloading has an effect and will decreases the DFIG power generation and has to be taken seriously for the wind energy conversion system so as to maintain power system load balancing.

3.3 Simplified wind turbine model for frequency studies

The change in frequency in any one area is dF, the low-pass filter time constant is T_r, washout parameters are T_{w1} and $1/R_1$ is conversion gain to convert to rotor speed. The rotor speed limited within lower and upper limits. For DFIG (0.6 to 1.3 p.u.) are speed limits for safe and better operation considering gearwheel and other turbine-generator set parameter

safety. The output of this speed gives the reference rotor speed value at that instant. The change in wind rotor speed is given by dw, here in our study, it is considered as constant and zero. The speed change error is given to PI controller and added to speed error reference parameter. The reference and actual speed are given with wind turbine time constant is (T_{a1}) gives the real power flow. The power flow is cut-off between minimum and maximum values and this is change in real power flow change. The sub-system model of DFIG wind energy conversion system for the load frequency response [22] is shown in Fig.1. The rotor speed lookup table and inertia parameters are also shown.
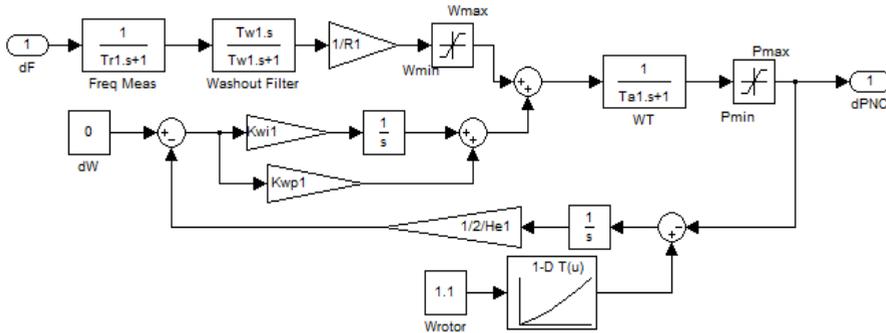

Fig.1 DFIG based sub-system model for load frequency control (LFC)

4. Two area test bed system and compensating devices design considered in our case study

4.1 Two area test bed system under study

The two area generation system for load frequency control study is shown in Fig.2a. This system is having two areas connected by a tie-line with equivalent impedance of transmission line as X_{12}. The current is expected to flow from area 1 to area 2. If due to load switching or generation scheduling, frequency, real power will change and reach a steady-state after certain oscillations based on these disturbances. To improve the oscillations damping FACTS devices are used. In are 1, the voltage is at angle $V_1\angle\delta_1$ and in area 2 is $V_2\angle\delta_2$. The angle injected/ absorbed by FACTS device is $1\angle\phi$, therefore voltage at bus 2 is $V_1\angle(\delta_1+\phi)$. This angle can be positive or negative based on disturbance and oscillation value. Based on the effective control of this angle Φ, that much effective the FACTS device. Each area consists of GENCO, load and WECS as shown in Fig. 2b. The WECS is a DFIG based system which will be dealt in next section.
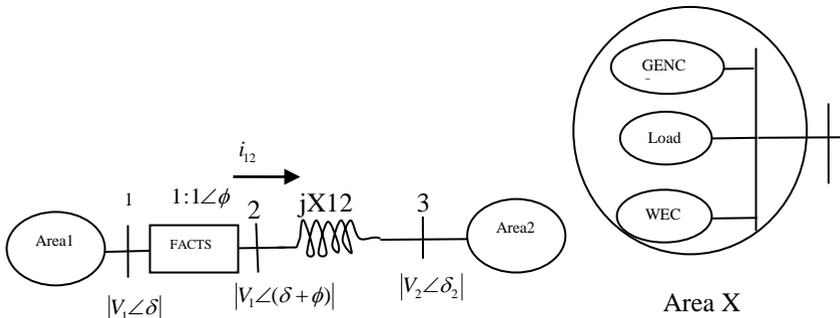

Fig.2a Two-area system under study with FACTS devices load schematic

Fig.2b one area source,

Due to the disturbance like load switching, there will be frequency oscillations as well as power oscillations. If frequency oscillations are not damped effectively, the system will collapse leading to reliability issues. If frequency regulation is improved, power oscillations are controlled effectively and further reactive power oscillations to certain extent. The real and reactive power and frequency oscillations can be mitigated using proper FACTS devices with its control strategy. Hence frequency regulation is important for real power and frequency oscillations damping. The two area LFC system with DFIG and SMES compensation is shown in Fig.3.
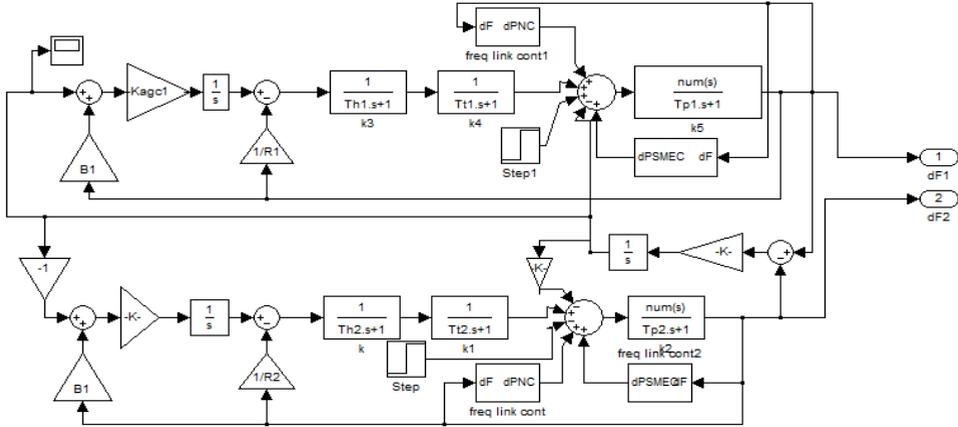

Fig.3 Two area system with DFIG and SMES storage system designed using MATLAB software

4.2 The design of SMES and FACTS devices

The SMES internal block diagrams are shown in Fig.4a and that of TCPS is shown in Fig. 4b(i) and its connection diagram to a network is shown in Fig.4b(ii) [16]. The SMES model is designed for a two area generation control is given by equation (19) [23]. This SMES storage device is costlier than battery and also requires more maintenance, has more losses, but is an effective device in terms of compensation of mostly reactive power and frequency. It is having more life time, quicker in action and takes lesser time for charging and discharging.

$$\Delta P_{tie12}(s) = \frac{2\Pi T_{12}}{s}\left(\Delta F_1(s) - \Delta F_2(s)\right) + K_f\left(\frac{1+T_1s}{1+T_2s}\right)\left(\frac{1+T_3s}{1+T_4s}\right)\left(\frac{K_{SMES}}{1+T_{SMES}s}\right)\Delta F_1(s) \quad (19)$$
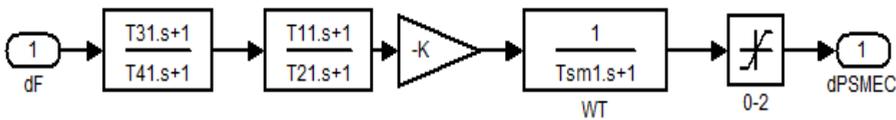
Fig.4a Internal block diagram of SMES designed in MATLAB software

The internal block diagram as a transfer function model and connection diagram of thyristor controlled capacitor storage phase shifters (TCPS) in a two area network is shown in Fig.4b(i) and Fig.4b(ii). The area-1 and area-2 voltage and its load angle is represented as V_1, $V2$ and θ_1 and θ_2, the compensating angle is ϕ_1. The TCPS for a two area system is represented by the equation (20) as

$$\Delta P_{tie12}(s) = \frac{2\Pi T_{12}}{s}\left(\Delta F_1(s) - \Delta F_2(s)\right) + T_{12}\left(\frac{K_\phi}{1+T_{TCPS}s}\right)\Delta F_1(s) \qquad (20)$$
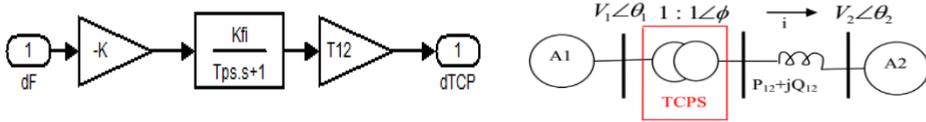
Fig.4b(i) Internal block diagram of TCPS and Fig.4b(ii) network diagram

The TCPS is one of the better FACTS devices which is connected in series to a network used for real power flow and frequency regulation in a power network. This device is cheaper than SMES, effective, promising, rapid in action, requires lesser maintenance and longer life. Compared to this SSSC is also a series device, is quicker than TCPS with longer life, better controllability even for a very large system. But it is more complex and costlier than TCPS. The equation (21) describes the power and frequency control operation in a tie-line and transfer function is in Fig.4c(i) and the network connection of SSSC to a two area system is shown in Fig.4c(ii).

$$\Delta P_{tie12}(s) = \frac{2\Pi T_{12}}{s}\left(\Delta F_1(s) - \Delta F_2(s)\right) + K_1\left(\frac{1+T_1 s}{1+T_2 s}\right)\left(\frac{1+T_3 s}{1+T_4 s}\right)\left(\frac{K_2}{1+T_{SSSC}s}\right)\Delta F_1(s) \qquad (21)$$
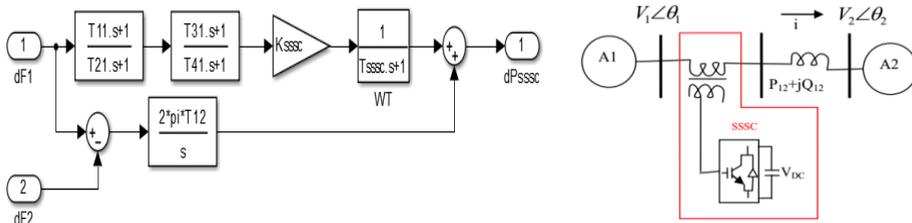
Fig.4c(i) Internal block diagram of SSSC and Fig.4c(ii) network diagram

The internal block diagrams of UPFC and IPFC are shown in Fig.4d(i) and 4d(ii). The UPFC is a single bus hybrid device with SSSC in series to the network and Static Compensator (STATCOM) as a shunt device. Hence, the performance of UPFC is better than SSSC as it is having it and also STATCOM. This makes the UPFC more costlier, complex, more requirement of maintenance, more floor space, and lesser reliable, but is more effective in frequency compensation, power loss control, power flow ability, improves stability and loadability limit and has better dynamic operation than any FACTS device that is connected in a single line. The interline power flow control (IPFC) is a two device single unit series device containing two SSSC devices in two lines or multiple lines. The IPFC is prevalent when compensation is required in more than a single transmission line. This IPFC is a better device than UPFC when voltage, real and reactive power flow, frequency, load angle, losses and stability of a system is considered in two lines, while UPFC will do for a single line. The equations describing the UPFC and IPFC tie-line frequency and power flow regulation can be expressed as in (22) and (23). The parameters and coefficients are shown in Appendix [13 and 16]

$$\Delta P_{UPFC}(s) = \left(\frac{1}{1+T_{UPFC}s}\right)\Delta F_1(s) \qquad (22)$$

$$\Delta P_{IPFC}(s) = \left(\frac{1}{1+T_{IPFC}s}\right)\left(K_1\Delta F_1(s) + K_2\Delta P_{12}(s)\right) \qquad (23)$$
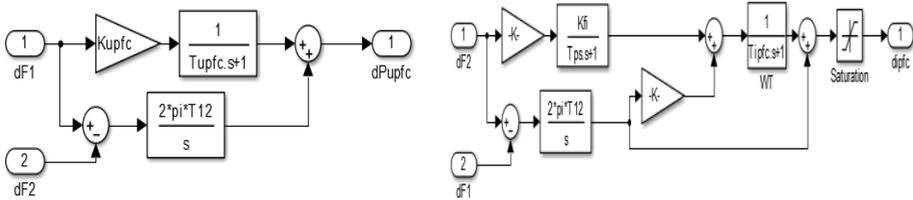

Fig.4d(i) Internal diagram of UPFC and Fig.4c(ii) Internal diagram of IPFC

5. Result Analysis

The influence of various FACTS devices and SMES connected to a circuit shown in Fig.2a is discussed in this section under three cases. The case-1 studies the operation of load change in area-1 at 1 second with SMES, TCPS and hybrid combination of both for a 0.1 p.u. increase and the effect of frequency change and effectiveness among these two are analyzed. In the case-2, performance of TCPS, SSSC, UPFC and IPFC are studied and their effectiveness is analyzed. Later in the third case, coordinated energy devices are planned in which two energy storage devices or FACTS devices are connected in parallel and the best combination among them is observed.
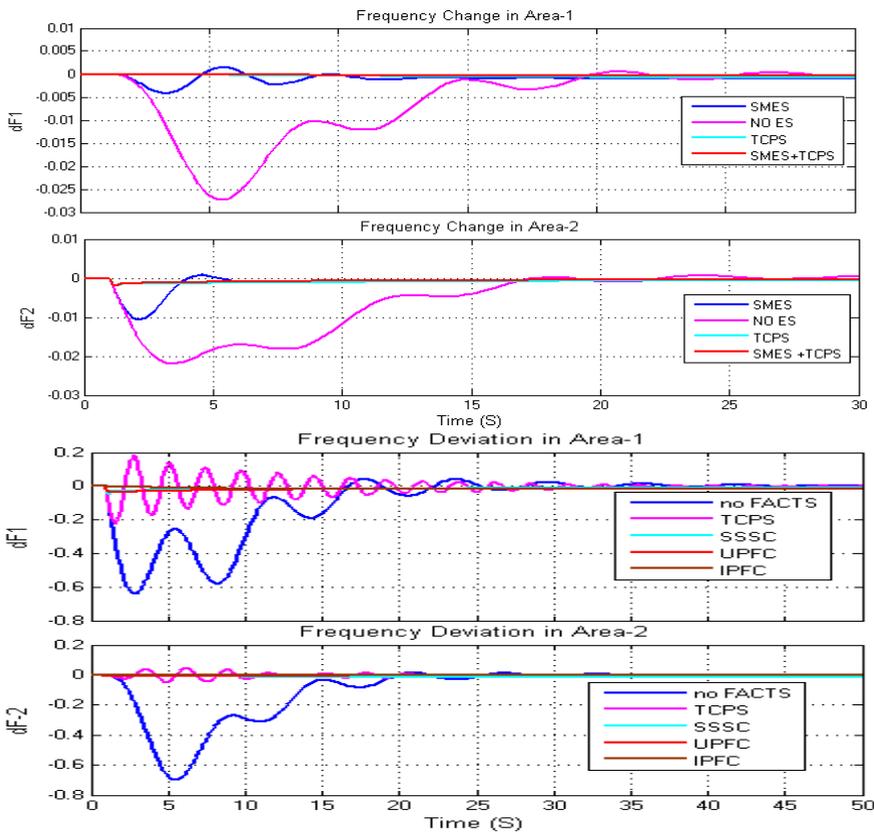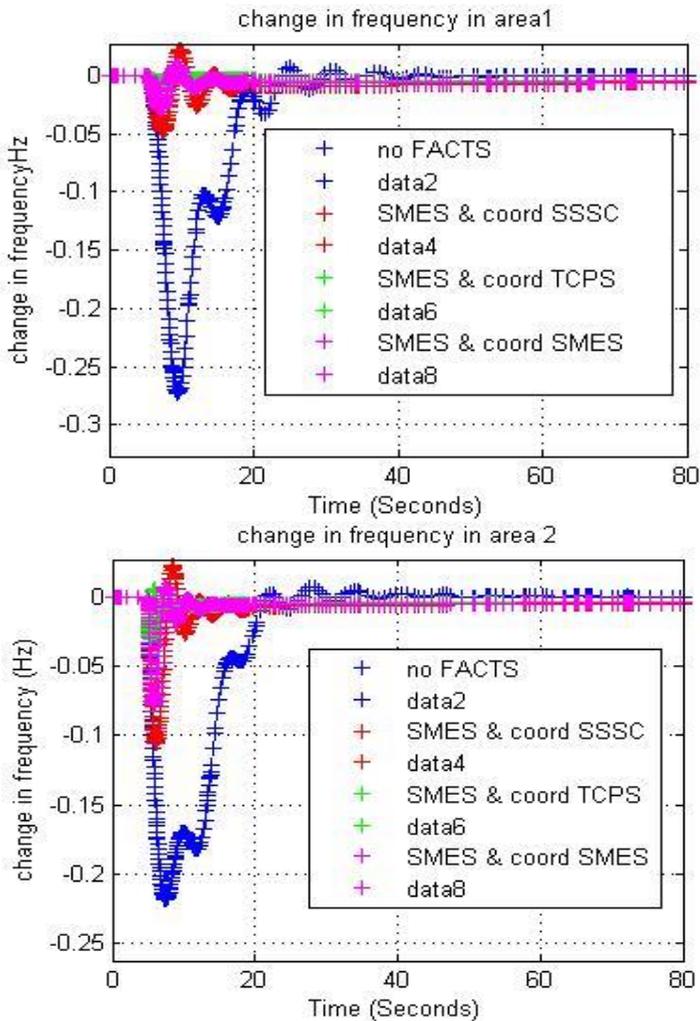

Fig. 5(i) Area-1 (top) and area-2 change in frequency under case-1 and Fig.5(ii) for case-2

In the case-1, the objective is to find the better device among SMES and TCPS, so almost same rating devices are considered for the same two area bus network. From the Fig.5(i), it is observed that the change in frequency in area-1 (top) without any energy storage device (NO ES) is having more deviation of -0.0275 p.u. while with SMES is having very small deviation with lesser oscillations and settled quickly. When TCPS and hybrid combination of TCPS and SMES is observed, the deviation in frequency is very lesser than with SMES, which is almost negligible even for a 10% change in load suddenly. When comparing TCPS and hybrid devices in this case, the hybrid device is very dynamic and quicker in response. Compared to area-1, the area-2 is having lesser frequency deviation and frequency response is quicker as load change is in area-1 only and its influence to certain extent is observed in area-2 as it is connected to a tie-line. Hence, hybrid system is best, next is TCPS and then SMES is better in operation.

For the case-2, TCPS, SSSC, UPFC and IPFC based FACTS devices are considered for the same bed system, but with 50% increase in the load. It can be seen in Fig.5(ii) such large load change in one area will persuade remaining areas connected to a tie-line. There is almost 0.6 p.u. change in the frequency, which is very dangerous to a system and it will trip the network with the help of frequency protection relays. The sustained oscillations are observed in area-1 (top) and area-2 (bottom) is with TCPS. The frequency deviation is controlled by changing its phase angle, as it is little lesser predominating, oscillations are observed. The oscillations with ±0.2 p.u. are with lesser frequency (or higher time period) with TCPS as is a device having resonating column elements like inductor and capacitor. As describes in equation (18), TCPS is like a lag compensator of 1st order system and its frequency of oscillations depends on its time constant and its amplitude depends on the gain constant.

Now, SSSC is compared for the analysis, it is a better device than TCPS and is a 3rd order system with higher performance characteristics and better dynamic response as in equation (19). Hence, a small deviation of 0.02 p.u. or 2% is observed at the instant of load change and completely became zero in 12s. The UPFC which is a combination of SSSC and UPFC is described with a single order transfer function, but with different arrangement of its closed loop and is having better time constant and gain values than SSSC. Hence, this UPFC with better closed loop and hybrid characteristics is performing better than SSSC with a deviation of 0.012 p.u. and settled in 8 seconds. Now, finally IPFC which is a dual-SSSC in both areas is found having 0.006 p.u. frequency deviation and settled in less than 5 seconds. Therefore, among all the devices, the IPFC is the best with least deviation to frequency with 50% rapid change in load and quicker in response.

As observed in thecase-2, among all the external devices, SMES is having inferior performance and then TCPS, SSSC, UPFC, and IPFC. When considering coordinated SMES along with TCPS, the overall performance is found to be the best. In the third case, the frequency deviation is observed under no external storage device, coordinated SMES and SSSC, SMES with TCPS and SMES with another same SMES. With SMES-SMES, the deviation is high as with pink color markings, with SMES - TCPS coordination as wit red color data, the deviation is better than SMES-SMES. with SMES – TECPS (with green color marking), the deviation is very small and system is completely stable and is better than other twio cases or with TCPS alone.

Fig. 6(i) Area-1 (top) and area-2 change in frequency under case-1 and Fig.6(ii) for case-2

6. Conclusion

In this paper, SMES, TCPS, SSSC, UPFC and IPFC are analyzed for a two area network with sudden load change in area-1 and the compensation characteristics of the devices are observed in both the areas. If in one area, there is a sudden change in the load, this load change in the other area is influenced as both the areas are connected to a tie-line network. A small deviation in load in one area may not change the frequency considerably in other area, but a large change in load will influence to a greater extent, that may trip both areas from the grid due to large frequency and power flow deviations. Hence, protection of the system and reliability are considered, these external energy or FACTS devices play a vital role in controlling a surge change in frequency or power flow deviation. Among all these devices considered, SMES is good, the better than this in performance increasing order is TCPS, SSSC, UPFC and the best device is IPFC. This IPFC is having more advantages than UPFC is lesser complex, lesser switching elements and can be connected to more lines with a cheaper price than UPFC. With basic primary, secondary and tertiary frequency control mechanism, the DFIG frequency reached to normal value after few

oscillations. With SSSC, frequency settling is better than with FACTS. But TCPS is better than SMES and is better than SSSC in controlling real power and frequency deviation. With coordinated FACTS- SMES, SMES and TCPS behavior is best, SMES-SSSC is better and SMES-SMES is good than without FACTS or SMES. Hence, along with basic frequency regulation, application of full rated TCPS or with half rated each with coordinated SMES-TCPS is a better option for LFC.

Appendix

Synchronous generator, DFIG and tie-line parameters: K_{agc1}=0.05; K_{agc2}=0.05; H_{e1}=3.5; H_{e2}=3.5; T_{12}=0.0866; K_{wi1}= 0.1; K_{wp1}=1.58; K_{wi2}=0.1; K_{wp2}=1.61; T_{t1}=1; T_{t2}=1; T_{w1}=6; T_{w2}=6; T_{a1}=0.2; T_{a2}=0.2; K_{p1}=12; K_{p2}=12; R_1=3; R_2=3;T_{h1}=0.1; T_{h2}=0.1; T_{p1}=10; T_{p2}=15; T_{r1}=0.1; T_{r2}=0.1;

SSSC parameters: K_{sssc}=15.91830; T_{sssc}=0.0815254; T_{11}=0.0814835; T_{21}=0.0815148; T_{31}=0.082393; T_{41}=0.081295. UPFC parameters: T_{upfc}=0.017801; K_{upfc}=1.0;

IPFC parameters: K_{ipfc1}=3.1270; K_{ipfc2}=3.12116; T_{ipfc}=0.006145.

SMES parameters: W_{max}=1.4; W_{min}=0.0; T_0=0.07; B_1=1.1; P_{max}=3; P_{min}=0; K=10.1378; T_{sm}=10.50; K_1=20.2188; T_{11}=0.587; T_{21}=0.158; T_{31}=0.0575; T_{41}=0.2316; T_{sm1}=0.2151;K_{fi}=24.9004; T_{ps}=0.0016172.

Reference

[1] Abdulraheem, Bashar Sabeeh, and Chin Kim Gan. "Power system frequency stability and control: Survey." *International Journal of Applied Engineering Research* 11, no. 8 (2016): 5688-5695.

[2] Falahati, Saber, Seyed Abbas Taher, and Mohammad Shahidehpour. "Grid secondary frequency control by optimized fuzzy control of electric vehicles." *IEEE Transactions on Smart Grid* 9, no. 6 (2017): 5613-5621.

[3] Annamraju, Anil, and Srikanth Nandiraju. "Coordinated control of conventional power sources and PHEVs using jaya algorithm optimized PID controller for frequency control of a renewable penetrated power system." *Protection and Control of Modern Power Systems* 4, no. 1 (2019): 1-13.

[4] Khooban, Mohammad-Hassan, Tomislav Dragicevic, Frede Blaabjerg, and Marko Delimar. "Shipboard microgrids: A novel approach to load frequency control." *IEEE Transactions on Sustainable Energy* 9, no. 2 (2017): 843-852.

[5] Dreidy, Mohammad, H. Mokhlis, and Saad Mekhilef. "Inertia response and frequency control techniques for renewable energy sources: A review." *Renewable and sustainable energy reviews* 69 (2017): 144-155.

[6] Pandey, Shashi Kant, Soumya R. Mohanty, and Nand Kishor. "A literature survey on load–frequency control for conventional and distribution generation power systems." *Renewable and Sustainable Energy Reviews* 25 (2013): 318-334.

[7] Veerasamy, Veerapandiyan, Noor Izzri Abdul Wahab, Rajeswari Ramachandran, Arangarajan Vinayagam, Mohammad Lutfi Othman, Hashim Hizam, and Jeevitha Satheeshkumar. "Automatic load frequency control of a multi-area dynamic interconnected power system using a hybrid PSO-GSA-tuned PID controller." *Sustainability* 11, no. 24 (2019): 6908.

[8] Jagatheesan, Kaliannan, B. Anand, Sourav Samanta, Nilanjan Dey, Amira S. Ashour, and Valentina E. Balas. "Particle swarm optimisation-based parameters optimisation of PID controller for load frequency control of multi-area reheat thermal power systems." *International Journal of Advanced Intelligence Paradigms* 9, no. 5-6 (2017): 464-489.

[9] Singh, Amita, Veena Sharma, and Vineet Kumar. "Meta-heuristic Approaches for Solving Automatic Generation Control Problems: A Brief Review." In *2018 IEEE 8th Power India International Conference (PIICON)*, pp. 1-4. IEEE, 2018.

[10] Bayati, Mostafa. "Using cuckoo optimization algorithm and imperialist competitive algorithm to solve inverse kinematics problem for numerical control of robotic manipulators." *Proceedings of the Institution of Mechanical Engineers, Part I: Journal of Systems and Control Engineering* 229, no. 5 (2015): 375-387.

[11] Mohamed, Emad A., and Yasunori Mitani. "Load frequency control enhancement of islanded micro-grid considering high wind power penetration using superconducting magnetic energy storage and optimal controller." *Wind Engineering* 43, no. 6 (2019): 609-624.

[12] AppalaNarayana, C. H., D. V. N. Ananth, KD Syam Prasad, C. H. Saibabu, S. Saikiran, and T. PapiNaidu. "Application of STATCOM for transient stability improvement and performance enhancement for a wind turbine based induction generator." *International Journal of Soft Computing and Engineering (IJSCE) ISSN* (2013): 2231-2307.

[13] Shankar, Ravi, S. R. Pradhan, Kalyan Chatterjee, and Rajasi Mandal. "A comprehensive state of the art literature survey on LFC mechanism for power system." *Renewable and Sustainable Energy Reviews* 76 (2017): 1185-1207.

[14] Shankar, Ravi, Ravi Bhushan, and Kalyan Chatterjee. "Small-signal stability analysis for two-area interconnected power system with load frequency controller in coordination with FACTS and energy storage device." *Ain Shams Engineering Journal* 7, no. 2 (2016): 603-612.

[15] Shankar, Ravi, Kalyan Chatterjee, and Ravi Bhushan. "Impact of energy storage system on load frequency control for diverse sources of interconnected power system in deregulated power environment." *International Journal of Electrical Power & Energy Systems* 79 (2016): 11-26.

[16] Ananth, D. V. N., GV Nagesh Kumar, D. Deepak Chowdary, and K. Appala Naidu. "Two area load frequency control for DFIG-based wind turbine system using modern energy storage devices." *Int. J. Pure Appl. Math* 114, no. 9 (2017): 113-123.

[17] Pappachen, Abhijith, and A. Peer Fathima. "Critical research areas on load frequency control issues in a deregulated power system: A state-of-the-art-of-review." *Renewable and Sustainable Energy Reviews* 72 (2017): 163-177.

[18] Rajbongshi, Rumi, and Lalit Chandra Saikia. "Performance of coordinated FACTS and energy storage devices in combined multiarea ALFC and AVR system." *Journal of Renewable and Sustainable Energy* 9, no. 6 (2017): 064101.

[19] Guerrero, Josep M., Juan C. Vasquez, José Matas, Luis García De Vicuña, and Miguel Castilla. "Hierarchical control of droop-controlled AC and DC microgrids—A general approach toward standardization." *IEEE Transactions on industrial electronics* 58, no. 1 (2010): 158-172.

[20] Vandoorn, Tine L., Juan C. Vasquez, Jeroen De Kooning, Josep M. Guerrero, and Lieven Vandevelde. "Microgrids: Hierarchical control and an overview of the control and reserve management strategies." *IEEE industrial electronics magazine* 7, no. 4 (2013): 42-55.

[21] Sedhom, Bishoy E., Magdi M. El-Saadawi, Ahmed Y. Hatata, and Abdulaziz S. Alsayyari. "Hierarchical control technique-based harmony search optimization algorithm versus model predictive control for autonomous smart microgrids." *International Journal of Electrical Power & Energy Systems* 115 (2020): 105511.

[22] Wang, Huaizhi, Yangyang Liu, Bin Zhou, Nikolai Voropai, Guangzhong Cao, Youwei Jia, and Evgeny Barakhtenko. "Advanced adaptive frequency support scheme for DFIG under cyber uncertainty." *Renewable Energy* (2020).

[23] Lal, Deepak Kumar, and A. K. Barisal. "Comparative performances evaluation of FACTS devices on AGC with diverse sources of energy generation and SMES." *Cogent Engineering* 4, no. 1 (2017): 1318466.